Journal of Medicinal Chemistry

pubs.acs.org/jmc

Article

Exendin 4-Hapten Conjugate Capable of Binding with Endogenous Antibodies for Peptide Half-life Extension and Exerting Long-Acting Hypoglycemic Activity

Shijie Dai, Haofei Hong, Kun Zhou, Kai Zhao, Yuntian Xie, Chen Li, Jie Shi, Zhifang Zhou, Lei Nie,* and Zhimeng Wu*

Cite This: *J. Med. Chem.* 2021, 64, 4947−4959

Read Online

ACCESS | Metrics & More | Article Recommendations | Supporting Information

ABSTRACT: Hapten-specific endogenous antibodies are naturally occurring antibodies present in human blood. Herein, we investigated a new strategy in which small-molecule haptens were utilized as naturally occurring antibody binders for peptide half-life extension. The glucagon-like peptide 1 receptor agonist exendin 4 was site-specifically functionalized with the dinitrophenyl (DNP) hapten at the C-terminus via sortase A-mediated ligation. The resulting Ex4−DNP conjugates retained GLP-1 receptor activation potency in vitro and had a similar in vivo acute glucose-lowering effect comparable to that of native Ex4. Pharmacokinetic studies and hypoglycemic duration tests demonstrated that the Ex4−DNP conjugates displayed significantly elongated half-lives and improved long-acting antidiabetic activity in the presence of endogenous anti-DNP antibodies. In chronic treatment studies, once-daily administration of optimal conjugate 7 demonstrated more beneficial effects without prominent toxicity compared with Ex4. This strategy provides a new approach and represents an alternative to the well-established peptide-Fc fusion strategy to improve the peptide half-life and the therapeutic efficacy.

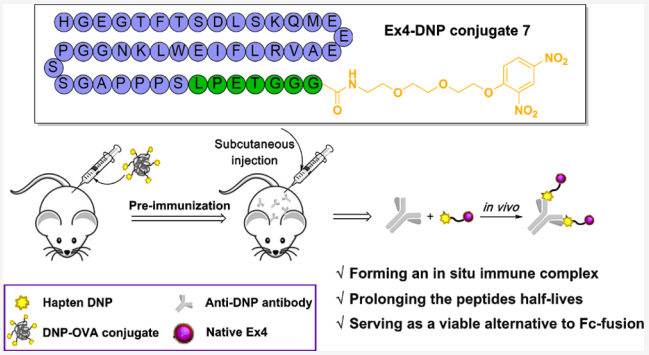

INTRODUCTION

Type 2 diabetes mellitus (T2DM) accounts for 90−95% of all diabetes cases and is defined as a progressive loss of adequate β-cell insulin secretion frequently in the context of insulin resistance.[1] Its prevalence has increased throughout both developed and developing countries over the past three decades, making this disease a key health priority globally.[2] Glucagon-like peptide 1 (GLP-1) and its analogues (e.g., exendin-4), as an incretin-targeting therapy, have been approved as an effective approach for T2DM treatment in recent years.[3,4] Mechanistic studies demonstrated that GLP-1 and its analogues stimulate the G protein-coupled glucagon-like peptide-1 receptor (GLP-1R) to enhance insulin secretion in a glucose-dependent manner through the cyclic adenosine monophosphate (cAMP) signal pathway.[5] Multiple beneficial effects, including slowing of gastric emptying, reduction of food intake and body weight, and improvement of pancreatic endocrine function, were also observed in this treatment.[6] However, one major challenge of using GLP-1-based peptide biologics as antidiabetes drugs in clinic is their relatively short half-life in vivo due to the inherent characteristics of the peptide, such as susceptibility to enzymatic degradation and rapid renal clearance; thus, they require high dosages and increased administration frequencies to achieve a therapeutic effect in clinic. To address this key issue, several elegant strategies have been successfully developed to increase the circulation time of GLP-1-based peptide drugs, such as peptide sequence optimization,[7,8] peptide post-translational modification with small functional molecules (e.g., lipidation[9,10] and dicoumarinization[11]), polymer conjugation (e.g., PEGylation[12] and carbohydrate conjugation[13,14]), protein fusion (album or Fc fusion), and sustained delivery systems. Generally, increasing the hydrodynamic radius by reducing renal elimination and steric shielding to reduce metabolic degradation are the two classical mechanisms of peptide half-life extension. To date, although the abovementioned strategies have achieved great success by generating several clinically approved GLP-1-based peptide drugs for T2DM treatment, there is still a significant demand to explore a novel strategy that includes a new mechanism to improve the peptide half-life and the therapeutic window and efficacy.

Received: January 8, 2021
Published: April 7, 2021

Scheme 1. Chemoenzymatic Synthesis of Ex4−DNP Conjugates 6−8 and FITC-Labeled Ex4−DNP Conjugates 9−11

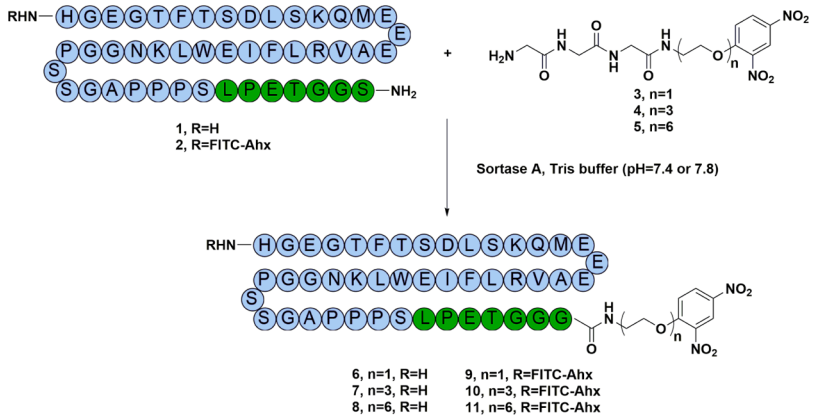

Of these strategies, genetically fusing peptides with antibody Fc fragments is an established approach to increase the circulation half-life of therapeutic peptides in the pharmaceutical industry.[15] Fusing the therapeutic peptide with the Fc fragment can not only provide steric hindrance from proteolysis but also reduce renal filtration by increasing the molecular weight. Importantly, the Fc domain in the fusion protein has been shown to mediate the neonatal Fc receptor (FcRn) salvage recycling pathway to further improve the serum half-life of peptide-Fc biologics.[16] Several Fc fusion peptide biologics have been clinically approved and are available on the market, including dulaglutide (Trulicity), etanercept (Enbrel), and aflibercept (Elyea).[17] However, the Fc fusion strategy also faces limitations and challenges. For example, peptide-Fc fusion therapeutic proteins are biomolecules that are usually produced by complex bacterial, yeast, or mammalian expression systems, and relatively expensive upstream and downstream processes are needed to obtain a pure and homogenous product for medical applications.[18] Another major concern is the potential immunogenicity elicited by frequent administration of peptide-Fc fusion drugs because these molecules are large and complex biologic counterparts compared with small molecules.[19,20] The generation of neutralizing anti-drug antibodies (nADAs) may diminish drug efficacy and induce severe adverse reactions as well.[21] For instance, 2.2% of patients were detected to have ADAs when treated with dulaglutide.[22]

Endogenous antibodies are naturally occurring antibodies present in human serum. A number of reports have documented that several antibodies against small-molecule haptens, such as galactose-α-1,3-galactose (α-Gal),[23] rhamnose,[24] and nitroarene,[25] exist in human blood abundantly, ranging from 1 to 8%.[24,26] Redirection of these endogenous antibodies with different isotype classes presents a variety of hapten-dependent biological functions.[27−30] For example, our group[29] and others[31] have demonstrated that small-molecule hapten-modified nanobodies or biotin can form in situ immune complexes with pre-existing endogenous antibodies, thus leading to significantly enhanced pharmacokinetic profiles. Moreover, small-molecule haptens, such as digoxin or cotinine, could be utilized as antibody binders to extend their circulatory half-lives or as a conjugate by forming immune complexes with the corresponding antibodies generated by a preimmunization approach in vitro or in vivo.[32,33] In this study, we proposed that small-molecule haptens may be utilized as naturally occurring antibody binders to extend the circulatory half-lives of peptide pharmaceuticals when conjugated with parent peptide drugs. Presumably, the rationally designed peptide−hapten conjugates could bind with pre-existing endogenous antibodies to generate a peptide−hapten−antibody complex that will prolong the half-life of the peptide following similar mechanisms as those of the peptide-Fc fusion strategy. However, a distinct feature of this approach, which is superior to the peptide-Fc fusion strategy, is that nonimmunogenic endogenous antibodies are harnessed; thus, it greatly avoids potential immunogenicity issues. As a proof of concept, GLP-1 analogue exendin 4 (Ex4) was selected as a model peptide to test the feasibility of this new strategy, while dinitrophenyl (DNP) hapten was selected as an endogenous antibody binder since naturally occurring anti-DNP antibodies are abundant in human blood across all genders, ethnicities, and ages.[34,35] C-terminal DNP-modified Ex4 analogues with different lengths of polyethylene glycol (PEG) as spacers were prepared by a well-established sortase A-mediated ligation method (SML).[36,37] The in vitro GLP-1R activation activity, in vivo acute glucose-lowering capability, long-term hypoglycemic activity, and in vivo pharmacokinetic properties of these conjugates were evaluated. Finally, the chronic treatment effect of a selected Ex4−DNP conjugate in db/db mice for a seven-week trial was described.

RESULTS

Design and Synthesis of Ex4−DNP Conjugates 6−8 and 9−11 via SrtA-Mediated Ligation. Ex4 is a clinically approved twice-daily peptide drug to treat T2DM. Previous studies have confirmed that the C-terminal modification of Ex4 has a limited impact on its potency. Thus, the C-terminus of native Ex4 was prolonged with a sorting signal motif (LPETGGS) that will conjugate with glycine-modified DNP hapten through a ligation reaction catalyzed by the transpeptidase sortase A (SrtA).[36,37] Three peptides, Ex4, Ex4-LPETGGS (1), and FITC-Ahx-Ex4-LPETGGS (2), were synthesized by standard solid-phase peptide synthesis (SPPS) procedures, further purified by semipreparative HPLC and characterized using MALDI-TOF or ESI MS and analytical HPLC (Figures S1−S6). Glycine-modified DNP derivatives 3, 4, and 5 containing different lengths of PEG were synthesized following our previous procedures.[29] Then, peptide 1 was incubated with 3, 4, or 5 in Tris buffer (pH = 7.4) in the presence of SrtA overnight to generate Ex4−DNP conjugates 6, 7, or 8 (Scheme 1). The reaction progress was monitored by RP-HPLC, as presented in Figure 1a−c, which shows that the

https://doi.org/10.1021/acs.jmedchem.1c00032
J. Med. Chem. 2021, 64, 4947−4959

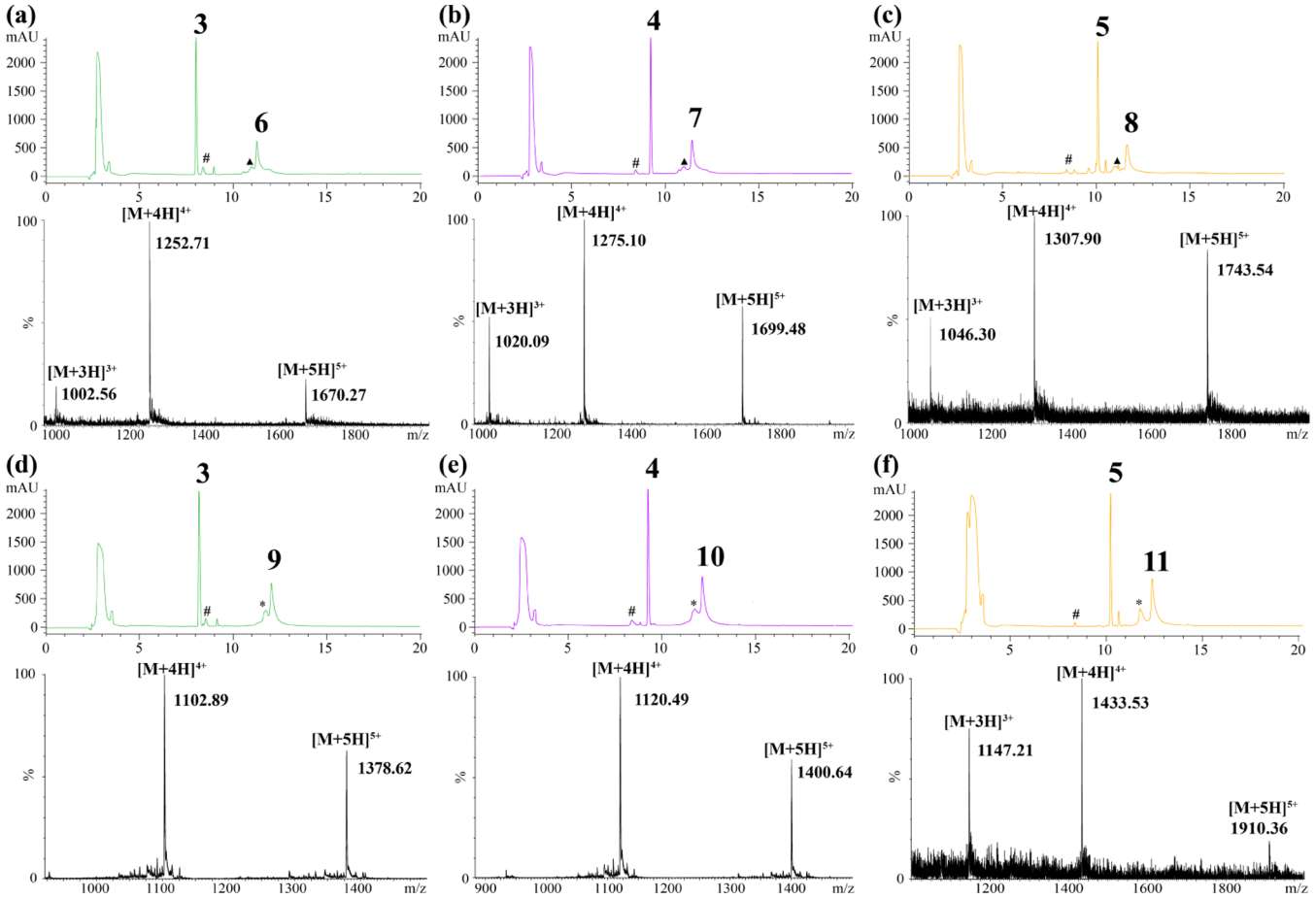

Figure 1. HPLC profile of SrtA-mediated ligation and ESI-MS analysis of 6 (a), 7 (b), 8 (c), 9 (d), 10 (e), and 11 (f). HPLC conditions: 10−90% gradient of CH_3CN/H_2O over 20 min at a flow rate of 1 mL/min and monitored at 220 nm (# represents SrtA; (▲) represents the unreacted peptide or hydrolysis product; and (*) represents the unreacted peptide 2 or hydrolysis product).

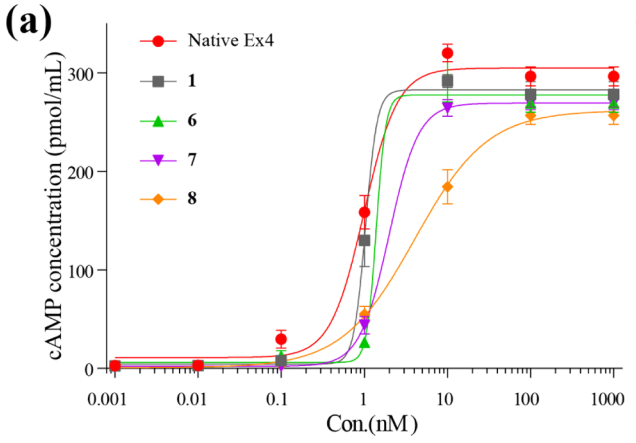

(b)

Compounds	EC_{50} (nM)	
	GLP-1R	SEM
Native Ex4	0.99	0.08
1	1.03	0.03
6	1.39	0.01
7	1.98	0.30
8	4.03	0.20

Figure 2. Activity was examined in vitro by measuring the cAMP response after receptor stimulation with native Ex4 and 1, and Ex4−DNP conjugates 6−8 in HEK293 cells that overexpressed human GLP-1R. (b) EC_{50} (nM) values of each compound against GLP-1 R derived from the cAMP response curve fitting. The results were described as the mean ± SEM, n = 3.

conversion yields were 80% for 6, 78% for 7, and 80% for 8. The ESI-MS analysis further confirmed that the conjugates were successfully synthesized. The reactions were scaled up to produce multiple milligrams of 6 (3.2 mg, 62% yield), 7 (3.1 mg, 60% yield), and 8 (3.0 mg, 57% yield) as a white powder after purification by semipreparative HPLC and lyophilization. The purities of conjugates 6−8 determined by analytic HPLC were over 95% (Figures S7−S9), which is suitable for biological studies. N-terminal FITC-labeled Ex4−DNP conjugates 9−11 were prepared following the same procedure and were characterized by ESI-MS (Figure 1d−f). These conjugates will be used for in vivo pharmacokinetic studies. It is worth noting that the optimal pH for the synthesis of conjugates 9−11 in the presence of SrtA should be adjusted to 7.8 because peptide 2 has poor solubility at pH 7.4.

https://doi.org/10.1021/acs.jmedchem.1c00032
J. Med. Chem. 2021, 64, 4947−4959

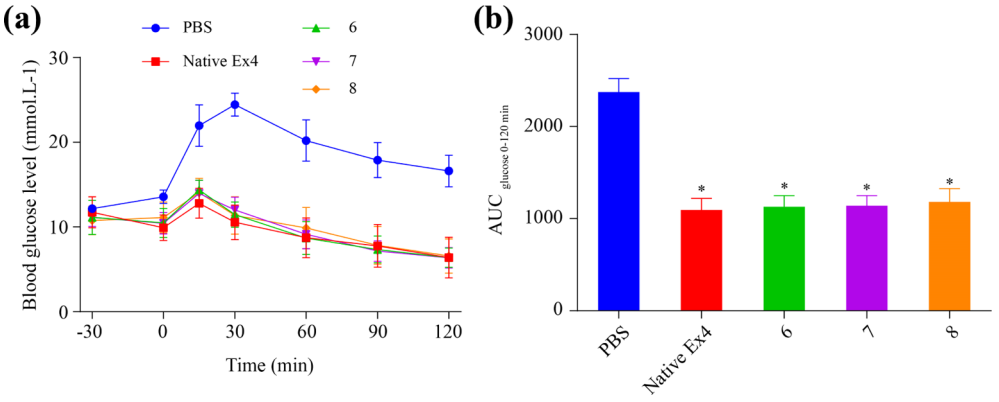

Figure 3. Glucose tolerance tests of PBS, native Ex4, and Ex4−DNP conjugates 6−8 (25 nmol/kg) in diabetic db/db mice. (a) Time response curves for the blood glucose level of each group. (b) Acute glucose-lowering effects are presented as calculated glucose $AUC_{glucose\ 0-120min}$ values. The results are depicted as the mean ± SEM (n = 5), *P < 0.05 vs the PBS group.

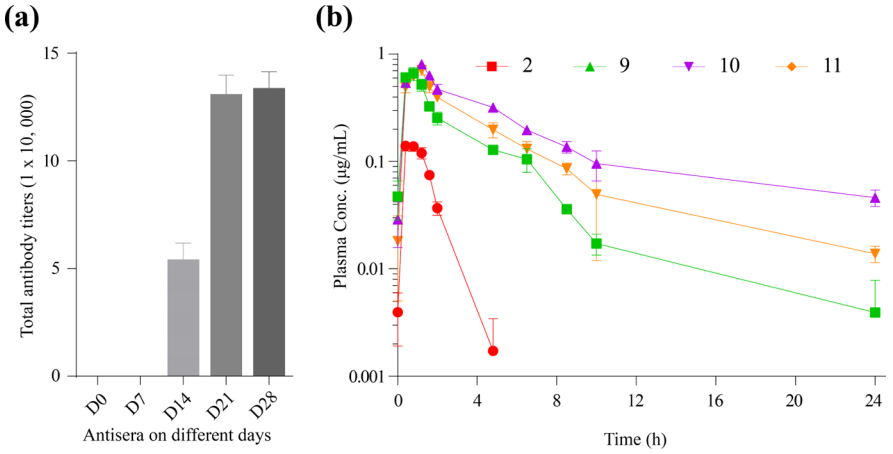

Figure 4. (a) ELISA results of total antibody titers of pooled antisera collected on different days from C57BL/6 mice immunized with DNP−OVA conjugates (n = 20). (b) Assessment of the pharmacokinetic properties of FITC-labeled native Ex4 (peptide 2) and Ex4−DNP conjugates 9−11 in preimmunized C57BL/6 mice subcutaneously administered with 75 nmol/kg FITC-labeled native Ex4. Blood samples were collected at various time points for fluorescence quantification. For peptide 2, the clearance rate after 6 h was not plotted because the plasma concentrations promptly fell below the quantification limit. A noncompartmental fit was applied to the data to deduce the pharmacokinetic parameters shown in Table 1. Results are depicted as the mean ± SEM, n = 5.

GLP-1 Receptor Activation Potency. GLP-1 and its analogues function by binding and activating GLP-1R, whose downstream signaling is mediated by a second messenger cAMP cascade and eventually results in the secretion of insulin to regulate blood glucose. Therefore, the level of cAMP is evaluated as an indicator of GLP-1R activation.[38] To examine whether Ex4 analogue 1 and its DNP-modified conjugates 6−8 retained the activity of GLP-1 receptor binding, we measured the intracellular cAMP levels by incubation of human embryonic kidney 293 (HEK293) cells that were stably transfected with human GLP-1R with various concentrations of the abovementioned peptides. As shown in Figure 2, both native Ex4 and 1 could significantly enhance intracellular cAMP levels in a concentration-dependent manner and displayed comparable EC_{50} values (0.99 nM vs 1.03 nM), which proved that extending the C-terminus of native Ex4 with a peptide motif (LPETGGS) did not significantly alter its receptor activation activity. Ex4−DNP conjugates 6, 7, and 8 exhibited slightly decreased potency in terms of stimulating GLP-1R compared with native Ex4 and 1, but the EC_{50} values remained at the nanomolar level (6: 1.39 nM; 7: 1.98 nM; and 8: 4.03 nM). Conjugate 8 displayed the worst receptor activation potency, indicating that a longer linker was not preferred in this modification (Figure 2).

Acute Glucose-Lowering Effect of Ex4−DNP Conjugates on Diabetic db/db Mice. To examine the glucose-regulating bioactivities of Ex4−DNP conjugates in vivo, IPGTT experiments were performed using $Lepr^{db}$ mutation C57BLKS/J db/db mice as a diabetes model. The experiments were performed by intraperitoneal injection with phosphate-buffered saline (PBS) and native Ex4 and Ex4−DNP conjugates 6−8 at a single dose of 25 nmol/kg of body weight. As illustrated in Figure 3a, the blood glucose levels of mice pretreated with PBS increased rapidly, reached peak values at 30 min (24.4 mmol/L) after glucose challenge (i.p., 1 g/kg), and maintained a state of hyperglycemia for 0−120 min, which was due to the impaired glucoregulatory function of the pancreas. However, groups treated with native Ex4 and Ex4−DNP conjugates 6, 7, and 8 showed rapid decreases in blood glucose levels to 12.8, 14.3, 13.9, and 14.0 mmol/L at 15 min after the same level glucose challenge (i.p., 1 g/kg), respectively, which gradually returned to baseline levels within 60 min. In addition, the AUC values of the blood glucose levels within 2 h after glucose challenge were reduced by 53.9%

https://doi.org/10.1021/acs.jmedchem.1c00032
J. Med. Chem. 2021, 64, 4947−4959

Table 1. Pharmacokinetic Parameters of Native Ex4 and FITC-Labeled Ex4−DNP Conjugates 9−11 in Preimmunized C57BL/6 Mice, Deduced from Data in Figure 4b

compounds	$T_{1/2}$ (h)	T_{max} (h)	C_{max} (μg/mL)	AUC (μg·h/mL)
native Ex4	0.72 ± 0.07	0.55 ± 0.09	0.16 ± 0.01	0.21 ± 0.02
9	2.07 ± 0.05	0.71 ± 0.15	0.74 ± 0.07	1.77 ± 0.12
10	3.55 ± 0.33	1.03 ± 0.10	0.81 ± 0.03	3.09 ± 0.17
11	2.62 ± 0.17	0.99 ± 0.16	0.78 ± 0.03	2.37 ± 0.10

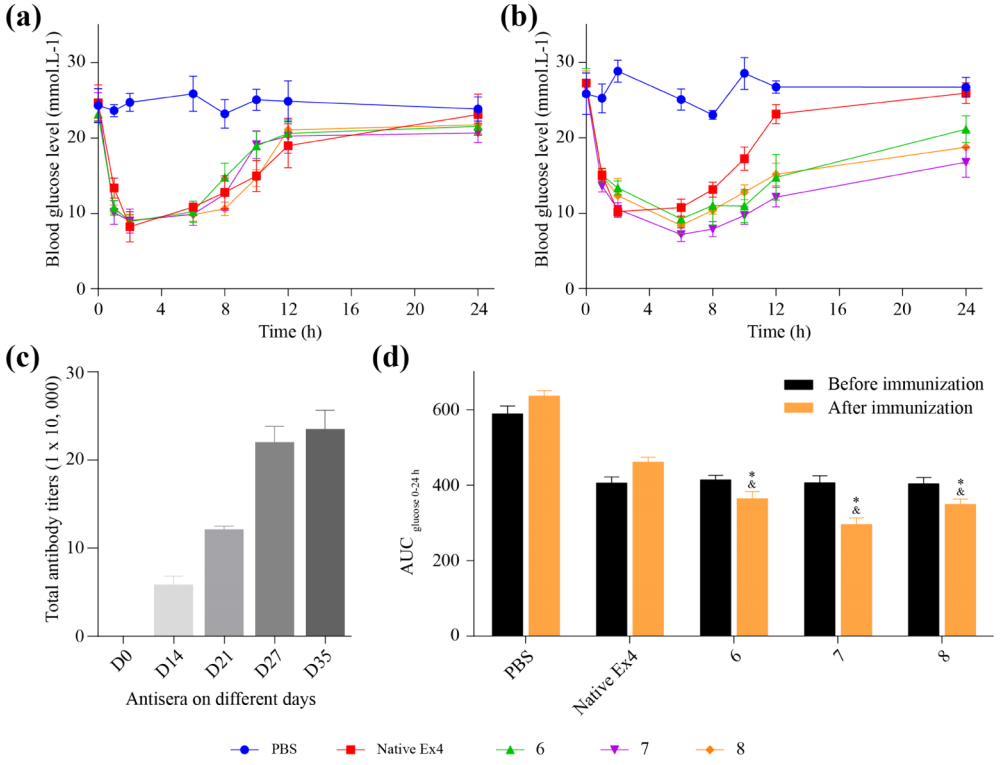

Figure 5. (a) Glucose-lowering profile in the db/db mouse model without anti-DNP antibodies in blood after subcutaneous injection of PBS, native Ex4, and Ex4−DNP conjugates 6−8 (25 nmol/kg, n = 5). (b) Glucose-lowering profile in the db/db mouse model with anti-DNP antibodies in blood after subcutaneous injection of PBS, native Ex4, and Ex4−DNP conjugates 6−8 (25 nmol/kg, n = 5). (c) ELISA results of total antibody titers of pooled antisera collected on different days from db/db mice immunized with DNP−OVA conjugates (n = 25). (d) Hypoglycemic effect of PBS, native Ex4, and Ex4−DNP conjugates 6−8 was calculated by the glucose AUC value between 0 and 24 h (n = 5). The results are depicted as the means ± SEM, $^{*}P < 0.05$ vs native Ex4 group, and $^{\&}P < 0.05$ vs Ex4−DNP conjugate 6−8 groups before immunization.

(native Ex4), 52.4% (6), 51.9% (7), and 50.3% (8) compared with those of the PBS group ($^{*}P < 0.05$), as presented in Figure 4b and Table S1. Thus, Ex4−DNP conjugates 6−8 exhibited similar glucose-regulating capabilities in vivo and were comparable to native Ex4, indicating that DNP modification of Ex4 did not impair its ability to promote insulin secretion bioactivities.

In Vivo Pharmacokinetic Study in C57BL/6 Mice Preimmunized with DNP−OVA. To validate our hypothesis that DNP-modified Ex4 conjugates can increase the in vivo half-lives through the interaction of DNP hapten with the corresponding endogenous anti-DNP antibodies, normal C57BL/6 mice were vaccinated with DNP−OVA conjugates to generate high titers of anti-DNP antibodies, as demonstrated by enzyme-linked immunosorbent assay (ELISA, Figure 4a). Then, pharmacokinetic studies were performed using FITC-labeled Ex4−DNP conjugates 9−11 at a dosage of 75 nmol/kg. The plasma concentration−time courses (Figure 4b) were analyzed using a noncompartmental fit to derive the pharmacokinetic parameters listed in Table 1. After a single subcutaneous injection, native Ex4 exhibited a very short residence time in circulation, which was expected, with a plasma $T_{1/2}$ value of 0.72 ± 0.07 h. In contrast, the plasma $T_{1/2}$ values of 9, 10, and 11 were 2.07 ± 0.05, 3.55 ± 0.33, and 2.62 ± 0.17 h, respectively, which represented 2.9-, 4.9-, and 3.6-fold increases relative to those of native Ex4. Interestingly, the peak plasma drug concentrations (C_{max}) of conjugates 9−11 in preimmunized mice were significantly improved and approximately 5-fold higher than those of native Ex4. These differences in the pharmacokinetics resulted in an approximately 8- to 15-fold increase in the AUC values for conjugates 9−11 compared with those of native Ex4. These data suggested that modification of Ex4 with hapten DNP could significantly prolong the half-life of the Ex4 peptide when abundant anti-DNP antibodies existed in the body. In addition, conjugate 10, which contained a medium-length PEG linker, possessed the best pharmacokinetic properties compared with other conjugates and native Ex4.

Long-Term Hypoglycemic Activity of Ex4−DNP Conjugates in Diabetic db/db Mice. Long-term hypoglycemic experiments were performed in diabetic db/db mouse models without or with anti-DNP antibodies in the blood. As

https://doi.org/10.1021/acs.jmedchem.1c00032
J. Med. Chem. 2021, 64, 4947−4959

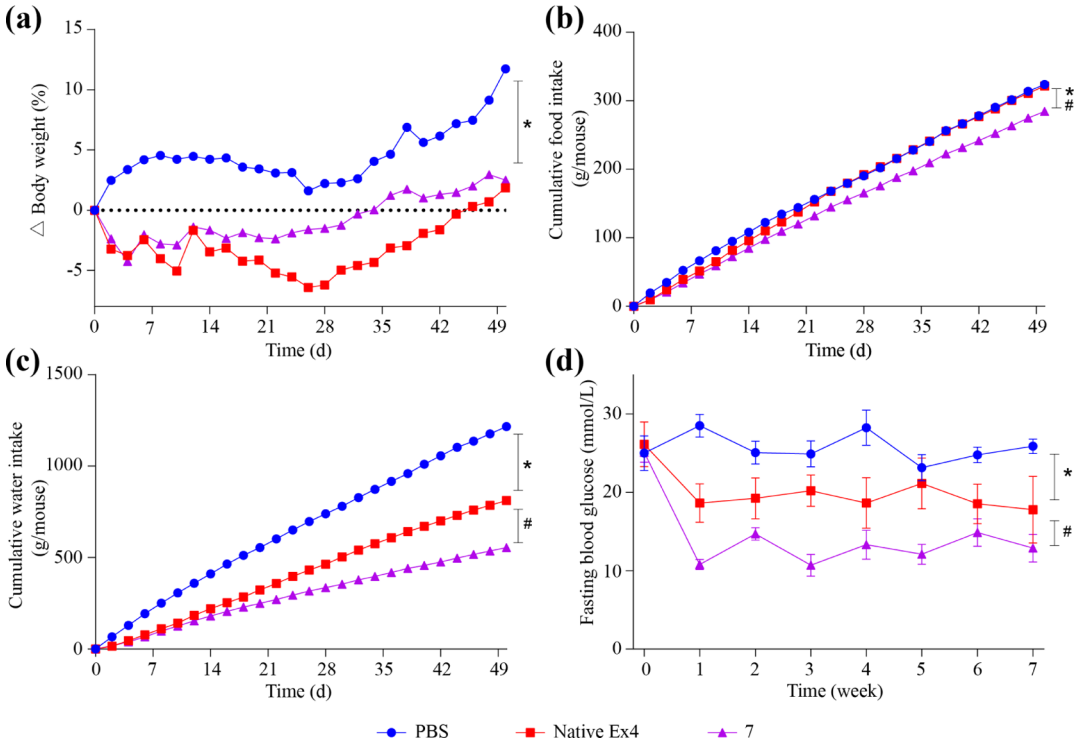

Figure 6. Effects of PBS, twice-daily native Ex4, and once-daily conjugate 7 by subcutaneous injection on (a) body weight, (b) food intake, (c) water intake, and (d) FBG (fasted for 8 h) levels during chronic treatment in preimmunized db/db mice. The results are depicted as the mean ± SEM (n = 5), *P < 0.05 vs the PBS group, and $^{\#}P$ < 0.05 vs the native Ex4 group.

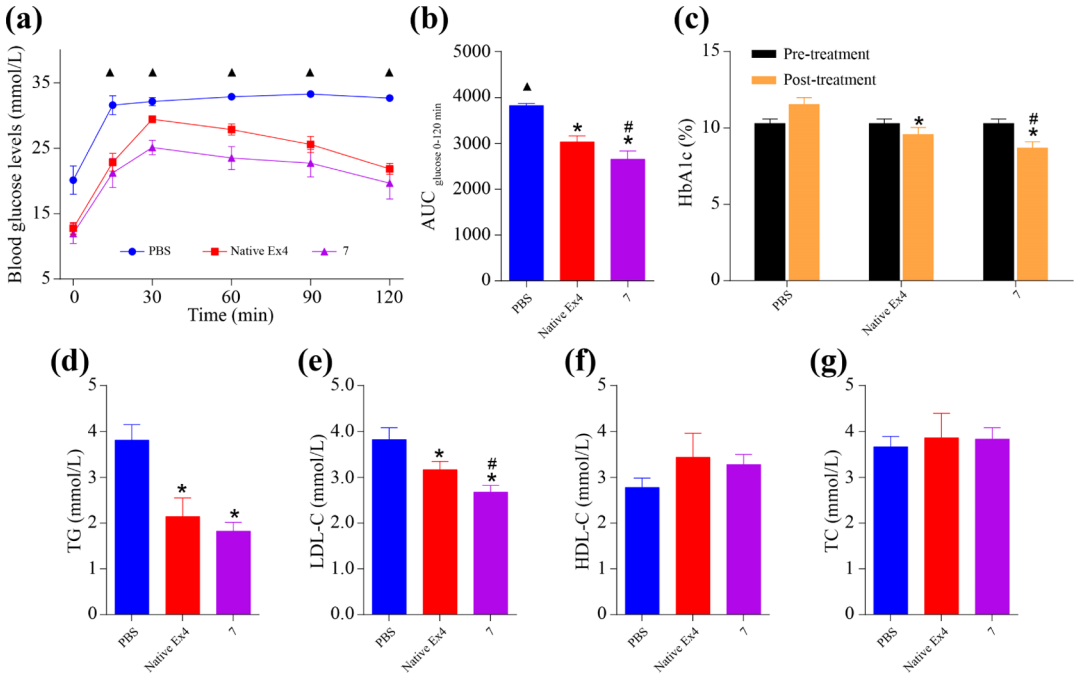

Figure 7. Chronic treatment effects of PBS, native Ex4, and conjugate 7 on glucose tolerance, HbA1c, and lipid metabolism indicators in preimmunized db/db mice. (a) Blood glucose excursion during IPGTT performed at the end of the chronic treatment. (b) AUC of IPGTT for 0−120 min after the administration of glucose (dosage of 0.5 g/kg). (c) HbA1c levels before and after chronic treatment. (d) Plasma TG, (e) LDL-C, (f) HDL-C, and (g) TC levels measured after the sacrifice of animals. The results are depicted as the mean ± SEM (n = 5), *P < 0.05 vs the PBS group, and $^{\#}P$ < 0.05 vs the native Ex4 group. (▲) Note: Since the range of the glucometer is 1−33.3 mmol/L, when the reading of the glucometer is displayed as "HI", maximal values of 33.3 mmol/L were substituted to enable statistical analysis.

illustrated in Figure 5a, in the diabetic db/db mouse model without anti-DNP antibodies in the blood, the mouse glucose level in the native Ex4 treatment group took 2 h to reach the lowest level and returned to the baseline level within 12 h. Ex4−DNP conjugates exhibited very similar glucose-lowering profiles as well. For the diabetic db/db mouse model with high

https://doi.org/10.1021/acs.jmedchem.1c00032
J. Med. Chem. 2021, 64, 4947−4959

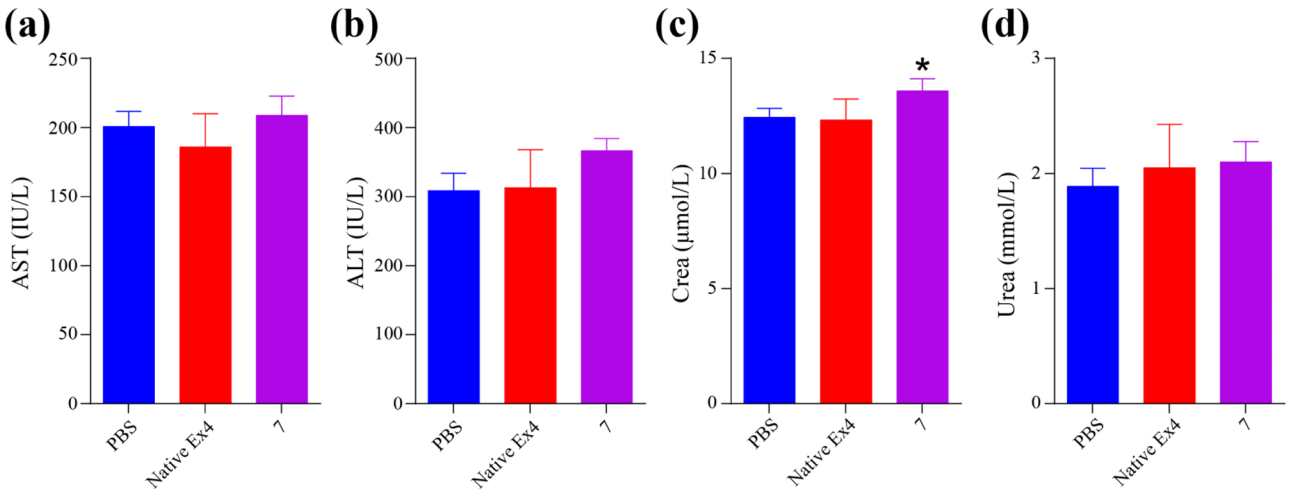

Figure 8. Toxicity effects of native Ex4 and conjugate 7 on the liver and kidney in preimmunized db/db mice after seven weeks of treatment. (a) AST, (b) ALT, (c) Crea, and (d) urea levels were measured by the corresponding assay kits on a BS-420 automatic biochemical analyzer after the sacrifice of animals. The results are depicted as the mean ± SEM (n = 5), *P < 0.05 vs the PBS group.

titers of anti-DNP antibodies in the blood, the native Ex4 treatment group displayed a glucose-lowering profile similar to that of the diabetic db/db mouse model. However, in this model, the mice's blood glucose levels in the conjugate 6−8 treatment groups decreased rapidly within 1 h and gradually reached the lowest levels in 6 h, and the blood glucose level still did not return to the baseline level even after 24 h of injection (Figure 5b). Compared with the PBS group, native Ex4 and Ex4−DNP conjugates 6−8 in the diabetic db/db mouse model without anti-DNP antibodies exhibited comparable $AUCs_{glucose\ 0-24h}$ values, which were 31.0, 29.7, 31.1, and 31.6%, respectively (Figure 5d and Table S1). In the diabetic db/db mouse model with high titers of anti-DNP antibodies, however, the $AUC_{glucose\ 0-24h}$ values of native Ex4 and Ex4−DNP conjugates 6−8 were reduced by 27.4, 42.8, 53.6, and 45.1% with significant differences (*P < 0.05), respectively. There were significant improvements in the $AUC_{glucose\ 0-24h}$ values between the Ex4−DNP conjugate administration groups in the two diabetic db/db mouse models (6: 29.7% vs 42.8%; 7: 31.1% vs 53.6%; and 8: 31.6% vs 45.1%, $^{\&}P$ < 0.05). These results demonstrated that the long-acting hypoglycemic activity was enhanced when Ex4 was modified with hapten DNP in the presence of anti-DNP antibodies. Among the Ex4−DNP conjugates, conjugate 7 containing a 3PEG linker was found to display the best long-term hypoglycemic effect, which was consistent with the results of previous pharmacokinetic experiments.

Chronic Treatment Effects of Ex4−DNP Conjugate 7. As Ex4−DNP conjugate 7 exhibited the best pharmacokinetic profile and superior long-term hypoglycemic duration activity among all DNP-modified Ex4 conjugates, it was selected to conduct a seven-week chronic treatment on preimmunized db/db mice. Based on the obtained pharmacokinetic profiles, conjugate 7 was administered once daily, while native Ex4 was given twice daily in these experiments.

Effect on Body Weight, Food Intake, Water Consumption, and Fasting Blood Glucose Levels. We monitored the body weight change, food intake, water intake, and fasting blood glucose (FBG) levels during the whole chronic treatment period. As shown in Figure 6a, both the native Ex4 and 7 treatments slowed the weight gain of the mice to a certain degree, especially in the initial intervention stage. At the experimental endpoint, mice in the native Ex4 and conjugate 7 groups showed a weight gain of approximately 1.9 and 2.4%, respectively, which was significantly different (*P < 0.05) from that of the PBS group (11.8% weight gain). In terms of the influence on food intake, Ex4−DNP conjugate 7 maintained a good inhibitory effect on mice throughout the chronic experiment, while native Ex4 only had a good inhibitory effect in the early stage (Figure 6b). Administration of native Ex4 and conjugate 7 significantly reduced water consumption and FBG levels during the whole experiment. Conjugate 7 exhibited obvious improvement effects over native Ex4 on the water consumption and FBG levels.

Effect on Glucose Tolerance, HbA1c, Lipid Metabolism, and Toxicity Indicators. IPGTT was performed at the endpoint of therapy in diabetic mice to investigate the glucose tolerance ability of each group after chronic treatment. As shown in Figure 7a,b, the $AUC_{glucose\ 0-120min}$ values of the native Ex4 and conjugate 7 groups were significantly decreased, showing improved glucose tolerance compared with those of the PBS group. By comparison of HbA1c levels before and after seven weeks of chronic treatment (Figure 7c), the HbA1c levels of the native Ex4- and conjugate 7-treated groups were decreased by 0.7 and 1.6%, respectively, but those of the PBS group were increased by 1.3%, indicating that both native Ex4- and conjugate 7-treated diabetic mice exhibited improved HbA1c levels. Notably, chronic administration of once-daily conjugate 7 improved glucose tolerance and reduced the HbA1c levels to a greater extent than the native Ex4 twice-daily injection treatment. Given the notable loss of body weight in the native Ex4 and conjugate 7 treatment groups, the indicators of lipid metabolism were also measured after chronic treatment. As illustrated in Figure 7d−g, native Ex4 and conjugate 7 significantly reduced the plasma LDL-C and TG levels of diabetic mice compared with the PBS group (*P < 0.05), and evaluations of HDL-C and TC levels did not reveal any substantial differences between groups. These results demonstrated that native Ex4 and conjugate 7 can improve lipid metabolism in db/db mice to a certain extent and the benefit of conjugate 7 treatments on lipid metabolism seemed to be better than that of native Ex4. In addition, toxicity indicators, such as hepatotoxicity (AST and ALT) and renal toxicity (Crea and urea), were measured (Figure 8a−d).

https://doi.org/10.1021/acs.jmedchem.1c00032
J. Med. Chem. 2021, 64, 4947−4959

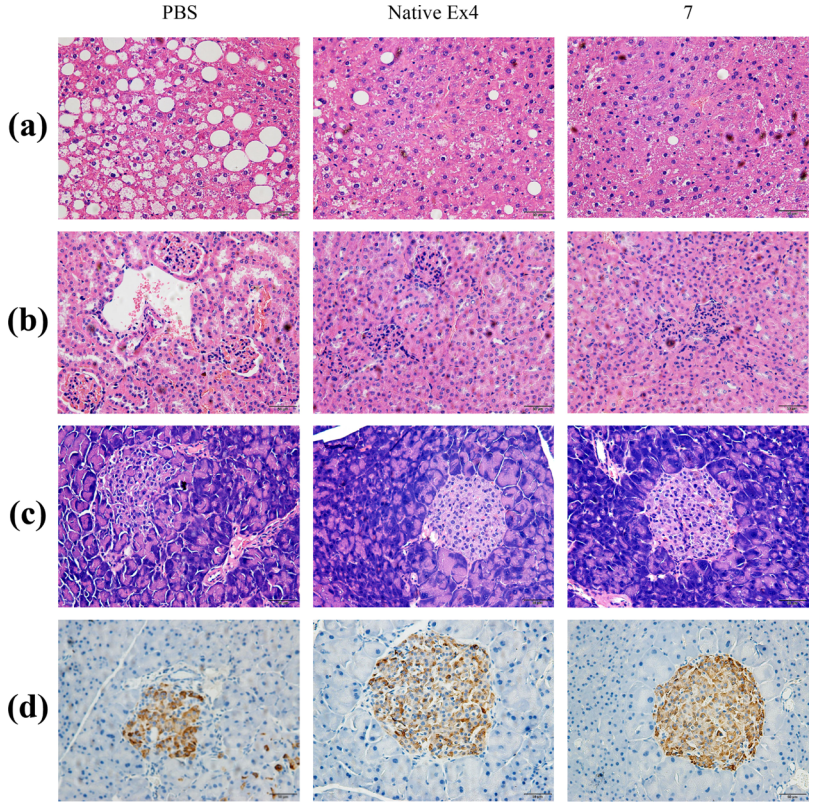

Figure 9. Protective effect of native Ex4 and conjugate 7 on the kidney, liver, and pancreas of db/db mice. Histological examination of the liver (a), kidney (b), and pancreas (c) sections with H&E staining. (d) Immunohistochemistry examination of pancreas sections with insulin antibodies. A denser color reflects more insulin secretion (scale bars = 50 μm).

The levels of the abovementioned toxicity indicators in the conjugate 7 treatment group were close to those in the PBS and native Ex4 groups, except that the Crea levels in the conjugate 7 groups were slightly higher than those of the PBS group. Taken together, these data proved that Ex4−DNP conjugate 7 did not show prominent toxicity effects during the seven-week treatment.

Histological Analyses and Immunohistochemistry. Finally, we performed H&E staining of the liver, kidney, and pancreas and immunohistochemistry analyses of the pancreatic islets of db/db mice after chronic treatment. As shown in Figure 9a,b, native Ex4- and conjugate 7-treated groups alleviated hypertrophy and empty cytoplasm in the liver and led to less structural alterations of the glomerular basement membrane in the kidney than the PBS group. More importantly, the pancreatic islets and acinus of pancreatic tissue samples in the conjugate 7 group were equally distributed and showed clear shapes and boundaries, which were much better than those of the PBS treatment group (Figure 9c). In the pancreas immunohistochemistry analysis, distinct positive signals to insulin were detected in the cytoplasm of endocrine islets. As indicated in Figure 9d, the area of insulin-positive β-cells in the conjugate 7 and native Ex4 treatment groups, which were stained brown, was obviously larger than that of the PBS group, indicating that both conjugate 7 and native Ex4 had notable protective effects on the pancreatic islets. Quantitative analysis of the insulin-positive cell area and the islet area revealed that conjugate 7 displayed the best insulin secretion effect, followed by native Ex4 and PBS (Figure S17).

DISCUSSION

The platform technology of recombinant fusion with the fragment crystallizable (Fc) domain of antibodies has been a widely used approach for the sustained delivery of peptide and protein therapeutics, as evident from several Fc fusion proteins approved by the FDA and more in clinical trials.[20,39] However, accumulated data have revealed that the Fc fusion strategy is still facing several intrinsic problems, such as complicated manufacturing processes, immunogenicity, and potential safety issues.[40,41] In this work, we took advantage of the small-molecule hapten, which serves as a naturally occurring endogenous antibody binder, to modify the native Ex4 peptide and increase its circulation half-life by the in vivo formation of the Ex4−hapten−antibody complex. The underlying mechanism of our strategy is quite similar to that of the Fc-fusion approach. Thus, this novel strategy can serve as a viable alternative to Fc fusion.

To site-specifically modify the C-terminus of Ex4, a well-established sortase A-mediated ligation was applied to synthesize Ex4−DNP conjugates. The conjugation of Ex4 analogue 1 with DNP derivatives was achieved in the presence of the biocatalyst sortase A with good conversion yields (approximately 80%). Three Ex4−DNP conjugates and their FITC-labeled Ex4−DNP conjugates with different lengths of PEG linker (n = 1, 3, 6) were obtained on a milligram scale. The GLP-1R activation abilities by the in vitro cAMP accumulation assay revealed that DNP modification at the C-terminus of Ex4 did not impair their biological activities dramatically, probably because the modification site is away from the N-terminus of Ex4, which is a crucial motif for receptor activation.[42,43] However, the activation potency was

https://doi.org/10.1021/acs.jmedchem.1c00032
J. Med. Chem. 2021, 64, 4947−4959

dependent on the length of the PEG linker in the conjugates, where a shorter PEG linker exhibited more potency. On the other hand, in vivo IPGTT experiments showed that the three conjugates displayed very similar acute glucose-lowering capabilities compared with those of native Ex4 since there was no significant difference in the calculated $AUC_{glucose\ 0-120min}$ values among the Ex4−DNP conjugates and native Ex4.

In the next PK studies (Figure 4) and hypoglycemic duration tests (Figure 5), three Ex4−DNP conjugates displayed improved pharmacokinetic properties in preimmunized C57BL/6 mice and improved long-acting hypoglycemic activity in preimmunized db/db mice compared with native Ex4. The degrees of improvement in the pharmacokinetic and pharmacodynamic properties of conjugates were related to the length of the PEG linker between DNP and native Ex4, in which conjugate 7 containing a 3PEG linker was superior to the other conjugates. Since Ex4−DNP conjugates can easily form an in situ immune complex with an abundance of endogenous anti-DNP antibodies in the blood, we speculated that DNP modification of therapeutic peptides is an alternative and convenient approach to improve the half-life through three known primary mechanisms: an increased hydrodynamic radius to prevent rapid renal clearance, reduced proteolysis by DPP-4, and an anti-DNP antibody Fc portion-directed FcRn-mediated recycling pathway. Therefore, our strategy can achieve the comparative benefits of the peptide-Fc fusion strategy through modification of the therapeutic peptide with hapten by a facile and convenient chemoenzymatic reaction. Meanwhile, the current approach could potentially avoid the immunogenicity issue caused by different allotypes of the Fc portion generated in the Fc-fusion strategy because biocompatible endogenous antibodies were involved in this strategy.

Finally, we conducted chronic treatment of preimmunized db/db mice to assess the potential therapeutic effect of Ex4−DNP conjugate 7. The long-term results show that once-daily administration of conjugate 7 delivered obvious beneficial effects on water and diet consumption and FBG levels compared with twice-daily administration of native Ex4 during the treatment period. More importantly, the glycosylated hemoglobin levels, glucose tolerance ability, and blood lipid levels of diabetic mice in the conjugate 7-treated group were significantly improved after continuous treatment for nearly 2 months compared with those of the native Ex4 group. In addition, no obvious toxicity effects were observed after chronic treatment with conjugate 7 on db/db mice, as determined by toxicity indicators. Finally, the histological results also suggested that conjugate 7 could reduce tissue injury and promote tissue repair of the kidney and liver, which were similar to the effects of native Ex4. The mouse sera from seven conjugate chronic treatment groups were pooled and analyzed by ELISA experiments using native Ex4 and Ex4−DNP conjugates 6−8 as capture antigens. The ELISA results are presented in Figure S16. The results showed that Ex4−DNP conjugates 6−8 could bind with the anti-DNP serum at high absorbance, indicating that a substantial amount of anti-DNP antibodies remained in the chronic treatment group. Notably, no absorption was observed in the Ex4 peptide coating group, which revealed that the mice treated with Ex4−DNP conjugate 7 did not produce detectable anti-Ex4 antibodies, even after nearly 2 months of treatment. This result strongly suggested that Ex4−DNP is essentially less or nonimmunogenic. The results of HE staining of the pancreas (Figure 9) and quantitative immunohistochemistry analyses for insulin in the pancreas sections (Figure S17) demonstrated that the once-daily administration of 7 has a significantly better improvement effect on islet function than twice-daily administration of native Ex4.

CONCLUSIONS

In summary, new GLP-1 analogues 6−8 with DNP modification at the C-terminus were efficiently synthesized by a chemoenzymatic method. In vitro GLP-1R activation studies and in vivo acute glucose-lowering experiments demonstrated that the resultant Ex4−DNP conjugates maintained similar potency and glucose-regulating capabilities as native Ex4. In PK and long-term hypoglycemic activity studies, the half-lives and long-acting antidiabetic activity of Ex4−DNP conjugates were remarkably improved in the presence of anti-DNP antibodies compared with those of native Ex4. In chronic treatment studies, once-daily administration of optimal Ex4−DNP conjugate 7 demonstrated superior therapeutic effects compared to twice-daily administration of native Ex4. Further investigations based on the structure of Ex4−DNP conjugate 7, such as introducing multivalent DNP or other haptens to enhance the interaction with endogenous antibodies, may lead to the development of once-weekly GLP-1 analogues. This strategy provides a new alternative to the peptide-Fc fusion strategy to improve the peptide half-life and therapeutic efficacy. Given the fact that peptide therapeutics are significantly growing in pharmaceutical industry,[44] our approach is conveniently amendable to other peptides.

EXPERIMENTAL SECTION

Materials. Fmoc-protected amino acids, Rink amide MBHA resin, 2-(1*H*-benzotriazole-1-yl)-1,1,3,3-tetramethyluronium tetrafluoroborate (TBTU), and 1-hydroxybenzotriazole (HOBt) were purchased from GL Biochem (Shanghai, China). FITC, trifluoroacetic acid (TFA), and triisopropylsilane (TIPS) were purchased from J&K Chemical Technology Co., Ltd. (Beijing, China). OVA (Cat. no. S25067), BSA (Cat. no. S12012), and HSA (Cat. no. S12018) were purchased from Shanghai Yuanye Bio-Technology Co., Ltd. (Shanghai, China). Dulbecco's modified Eagle Medium (DMEM, Cat. no. SH30243.01), fetal bovine serum (FBS, Cat. no. SH30084.03), penicillin−streptomycin solution (Cat. no. SV30010), and 0.25% Trypsin−EDTA (Phenol Red, Cat. no. SH30042.01) were purchased from GE Healthcare (Chicago, US). HRP-labeled goat anti-mouse IgG antibody (Cat. no. A0216), HRP-labeled goat anti-rabbit IgG antibody (Cat. no. A0208), and TMB solution (for ELISA, Cat. no. P0209) were purchased from Beyotime (Shanghai, China). The HbA1c assay kit (Cat. no. 044618002), TC assay kit (Cat. no. 141620003), LDL-C assay kit (Cat. no. 142019006), HDL-C assay kit (Cat. no. 142119010), and TG assay kit (Cat. no. 141719008), urea assay kit (Cat. no. 141318005), Crea assay kit (Cat. no. 141119010), AST assay kit (Cat. no. 140218005), and ALT assay kit (Cat. no. 140120005) were purchased from Shenzhen Mindray Bio-Medical Electronics Co., Ltd. (Shenzhen, China). All other reagents were obtained from commercial sources if not otherwise indicated.

Peptide Synthesis of Native Ex4 and Its Analogues 1 and 2. All peptides were prepared by SPPS on Rink amide resin (loading: 0.227 mmol/g, 0.05 mmol scale) using a CEM Liberty Blue automatic microwave peptide synthesizer (CEM Corporation, USA), as described in previous research.[14] In the process of synthesizing native Ex4 and its analogue peptides 1−2 (native Ex4: HGEGTFTSDLSKQMEEEAVRLFIEWLKNGGPSSGAPPPS, 1: HGEGTFTSDLSKQMEEEAVRLFIEWLKNGGPSSGAPPPS-LPETGGS, 2: FITC-Ahx-HGEGTFTSDLSKQMEEEAVRLFIEWLKNGGPSSGAPPPS-LPETGGS), 5 equiv of Fmoc-amino acids (dissolved in DMF), 10

https://doi.org/10.1021/acs.jmedchem.1c00032
J. Med. Chem. 2021, 64, 4947−4959

equivalents of DIPEA (dissolved in NMP), and 5 equiv of the activator (dissolved in DMF) were added together to conduct condensation reactions under microwaves of recommended parameter power in each coupling cycle. Deprotection of the N-terminal Fmoc group was performed using piperidine/DMF (20%, v/v). Since the coupling efficiency decreased with the prolongation of the peptide fragment, the coupling of the amino acids Ile^{21}, $Ala1^{7}$, and Glu^{16} was performed twice according to the prediction by amino acid condensation software in the peptide synthesizer. According to previous studies,[45] the deprotection of Asp^{9} was conducted in 20% piperidine (containing 0.1 mol·L^{-1} HOBT), and the coupling of Ser^{8} and His^{1} was conducted in TBTU (containing equivalent HOBT) by lowering the reaction temperature to 50 °C. For coupling with FITC, the condensation reaction was performed twice manually under 10 equiv of DIPEA without other activators. After completion of synthesis, the resin was treated with a cleavage mixture of TFA/H2O/TIPS (95:2.5:2.5, v/v/v) for 2 h at room temperature. The crude peptides were centrifuged and triturated with cold ether to obtain a suspension, followed by semipreparative HPLC purification (Agilent 1260 Infinity II) using an XBridgeTM Prep C18 column (250 mm × 10 mm, 5 μm, 130 Å). The molecular weights of native Ex4 and its analogues 1−2 were confirmed by matrix-assisted laser desorption/ionization time of flight mass spectrometry (MALDI-TOF-MS, ultrafleXtreme, Bruker Daltonics Inc., USA) or electrospray ionization mass spectrometry (MALDI SYNAPT mass spectrometer, Waters, USA). The purity of native Ex4 and its analogues 1−2 was determined by analytical HPLC (Agilent 1260 infinity) using a Diamonsil C18 column (250 mm × 4.6 mm, 3.5 μm, 100 Å) and confirmed to be ≥95% purity for all peptides based on the UV absorption at 220 nm. The results are shown in the Supporting Information, Figures S1−S6.

Synthesis of DNP Derivatives 3−5. Small DNP derivatives 3−5 were synthesized following our previous procedures.[29]

Reaction of Native Ex4 Analogues 1 or 2 with DNP Derivatives via SrtA-Mediated Ligation. Analogues 1 or 2 (1.0 μmol, 1.0 equiv), DNP derivatives 3, 4, or 5 (5 μmol, 5 equiv), and SrtA (6 μM) were dissolved in 2 mL of Tris buffer (50 mM Tris, 150 mM NaCl, 10 mM $CaCl_2$, pH = 7.4 or 7.8).[46] The reaction mixture was stirred at 30 °C overnight. After completion of the reaction as monitored by analytical HPLC, the reaction solution was quenched by the addition of 0.1% TFA aqueous solution. Purification was performed by semipreparative HPLC followed by concentration at reduced pressure and lyophilization to obtain pure Ex4−DNP conjugates 6−8 and FITC-labeled Ex4−DNP conjugates 9−11. Analytical HPLC results revealed that the purities of all conjugates were ≥95%, as determined by UV absorption at 220 nm (Supporting Information, Figures S7−S12). The ESI was calculated for $C_{218}H_{329}N_{59}O_{75}S$ (6) $[M + 3H]^{3+}$ m/z = 1669.46, $[M + 4H]^{4+}$ m/z = 1252.34, and $[M + 5H]^{5+}$ m/z = 1002.08, and the result was 1669.62; 1252.20; and 1002.56, respectively; for $C_{222}H_{337}N_{59}O_{77}S$ (7) $[M + 3H]^{3+}$ m/z = 1698.81, $[M + 4H]^{4+}$ m/z = 1274.36, and $[M + 5H]^{5+}$ m/z = 1019.68, and the result was 1698.80; 1274.36; and 1020.47, respectively; for $C_{228}H_{349}N_{59}O_{80}S$ (8) $[M + 3H]^{3+}$ m/z = 1742.83, $[M + 4H]^{4+}$ m/z = 1307.38, and $[M + 5H]^{5+}$ m/z = 1046.10, and the result was 1742.51; 1307.14; and 1046.30, respectively; for $C_{245}H_{351}N_{61}O_{81}S_2$ (9) $[M + 4H]^{4+}$ m/z = 1377.87 and $[M + 5H]^{5+}$ m/z = 1102.50, and the result was 1377.87 and 1102.49, respectively; for $C_{249}H_{359}N_{61}O_{83}S_2$ (10) $[M + 4H]^{4+}$ m/z = 1399.88 and $[M + 5H]^{5+}$ m/z = 1120.11, and the result was 1400.14 and 1120.10, respectively; and for $C_{255}H_{371}N_{61}O_{86}S_2$ (11) $[M + 3H]^{3+}$ m/z = 1910.20, $[M + 4H]^{4+}$ m/z = 1432.90, and $[M + 5H]^{5+}$ m/z = 1146.52, and the result was 1910.36; 1433.04; and 1146.41, respectively.

In Vitro cAMP Accumulation Assay. Human embryonic kidney 293 cells stably expressing the human GLP-1 receptor (GLP-1R) were used to evaluate the potency of native Ex4 and Ex4−DNP conjugates to active GLP-1R by determining cAMP production.[47] In brief, cells in the exponential growth stage were resuspended in DMEM with 2% FBS and seeded into 96-well microplates at a density of 2×10^4/well. After adhering overnight, cells were treated with 0.5 mM 3-isobutyl-1-methylxanthine (IBMX, J&K Chemical Technology, Beijing, China) for 40 min to avoid cAMP degradation, followed by incubation with native Ex4 or Ex4−DNP conjugates diluted in blank DMEM medium to concentrations within the 10^{-3} to 10^3 nM range for 20 min. Then, the cells were lysed with lysis buffer and centrifuged at 600*g* for 10 min at 2−8 °C to remove cellular debris. The intracellular cAMP levels were assayed using competitive cAMP ELISA according to the manufacturer's instructions (R&D Systems Inc, Minneapolis, MN, USA). Each sample was tested in triplicate, and the in vitro potency of each sample was quantified by determining the half-maximal effective concentration (EC_{50}) using GraphPad Prism version 6.0 (San Diego, USA).

In Vivo Pharmacokinetic (PK) Study. *Immunization of Normal C57BL/6J Mice to Generate Anti-DNP Antibodies in Serum.* A total of 20 female C57BL/6J mice (4 weeks old, 15 ± 2 g) were purchased from Shanghai Slac Laboratory Animal Co., Ltd. (Shanghai, China). On arrival, the mice were first housed and kept in the Animal Experimental Center of Jiangnan University for one week. The DNP−OVA conjugate (2 mg/mL) dissolved in PBS was mixed with alum adjuvant (Cat. no. 77161, Thermo) in an equal volume, followed by adequate shaking on a vortex mixer to prepare the vaccine formulations. Each mouse was inoculated on day 0 by intramuscular (i.m.) injection of 0.1 mL of the abovementioned vaccine formulations and enhanced 3 times on days 7, 14, and 21 by subcutaneous (s.c.) injection. Blood samples were collected on day 0 prior to the initial immunization and on days 7, 14, 21, and 28 one week after each immunization. The blood was centrifuged to obtain antisera, and the anti-DNP serum titers were determined by ELISA according to previous protocols.[48] During the entire animal experiment, mice were housed under controlled light on a 12 h light/12 h dark cycle with free access to food and water unless otherwise noted. All animal care and experimental procedures were approved by the Institutional Animal Care and Use Committee of Jiangnan University (JN. No20191115c0300117 [317]).

Pharmacokinetic Determination of Ex4−DNP Conjugates. The abovementioned immunized C57BL/6J mice were randomly divided into four groups (n = 5). Mice were weighed before injection. Each group of mice received a single subcutaneous injection of FITC-labeled native Ex4 and Ex4−DNP conjugates at a dosage of 75 nmol/kg. Each blood sample (20 μL) was obtained from the leg veins and using a pipette added into 80 μL of PBS solution (containing EDTA) at 40 s, 25 min, 50 min, 1.2 h, 1.6 h, 2 h, 4.8 h, 6.5 h, 8.5 h, 10 h, and 24 h after injection. Diluent blood samples were centrifuged at 4 °C and 3000 rpm for 15 min to extract the plasma for fluorescence reading at excitation 485 nm and emission 528 nm on a multifunctional microplate reader (synergy H4, Biotek). The plasma concentrations of each sample as a function of time were plotted using Prism 6 (GraphPad Software Inc.), and their pharmacokinetic parameters were estimated using WinNonlin Professional Version 6.0 (Pharsight Corp., Mountain View, CA, USA).

In Vivo Hypoglycemic Experiment. *Immunization of db/db Mice to Generate Anti-DNP Antibodies in Serum.* $Lepr^{db}$ mutation db/db mice (C57BL/6 background, male, 6−7 weeks) were purchased from the Model Animal Research Center of Nanjing University. On arrival, the mice were first housed and kept in the Animal Experimental Center of Jiangnan University for one week. Then, the mice were immunized with an emulsion of DNP−OVA conjugates and alum adjuvant (Cat. no. 77161, Thermo, 1 mL) to generate anti-DNP antibodies in serum according to the abovementioned procedure. All animal care and experimental procedures were approved by the Institutional Animal Care and Use Committee of Jiangnan University (JN. no. 20200430db0150825[004]).

Intraperitoneal Glucose Tolerance Test (IPGTT). The acute glucose-lowering activity of native Ex4 and Ex4−DNP conjugates was measured by IPGTT on db/db mice (n = 5). Before the experiment, mice were fasted for 18 h. Thirty minutes after intraperitoneal administration of each sample, the mice received the glucose challenge by intraperitoneal injection of 1 g/kg glucose. The second 1−2 μL of blood drop was collected by nicking the tail vein, and the glucose level was measured at −30, 0, 15, 30, 60, 90, and 120 min using a one-touch glucometer (Sannuo, Changsha, China). The

https://doi.org/10.1021/acs.jmedchem.1c00032
J. Med. Chem. 2021, 64, 4947−4959

area under the curve (AUC) of the blood glucose profiles was calculated for the period from 0 to 120 min with respect to the 0% baseline.

Hypoglycemic Duration Test. The long-acting antidiabetic effect of native Ex4 and Ex4−DNP conjugates was assessed in db/db mice (n = 5) using a previously described method.[49] Under nonfasting conditions with free access to water and food, mice were administered PBS, native Ex4, and Ex4−DNP conjugates (25 nmol/kg, s.c.). The second 1−2 μL of blood drop was collected via a cut of the tail tip to determine the blood glucose levels at 0, 1, 2, 6, 8, 10, 12, and 24 h using a one-touch glucometer (Sannuo, Changsha, China). The AUC of the glucose profiles was calculated for the period from 0 to 24 h with respect to the 0% baseline.

Chronic In Vivo Studies and Histological Analyses. To test the sustained therapeutic effect of conjugate 7 with the best performance on the PK study and hypoglycemic duration test, a chronic treatment experiment was performed on the abovementioned preimmunized db/db mice that possessed high anti-DNP antibody titers in the body. All db/db mice were assigned into three groups (n = 5) based on the fasting glucose levels. Mice in the positive control group and blank control group were subcutaneously administered native Ex4 and the same volume of PBS twice daily (9 am and 5 pm). Mice in the experimental group were subcutaneously administered conjugate 7 once daily. The glycated hemoglobin (HbA1c) levels of mice in each group were determined at the beginning and end of the chronic experiment using the corresponding assay kits on a BS-420 automatic biochemical analyzer (Mindray, Shenzhen, China). The FBG levels (fasted for 8 h) of each group were measured weekly by nicking the tail vein using a one-touch glucometer (Sannuo, Changsha, China). The amounts of food intake, water consumption, and body weight were recorded daily during the entire treatment. At the end of the chronic experiment, IPGTT was performed to determine the glucose tolerance. Specifically, following 18 h of fasting, mice were injected intraperitoneally with glucose (0.5 g/kg) at 0 min, and the blood glucose levels were determined at 0, 15, 30, 60, 90, and 120 min. Finally, all mice fasted overnight were sacrificed to collect blood samples by extracting eyeballs with EDTA to prevent blood from clotting. After centrifugation, the plasma levels of alanine aminotransferase (ALT), aspartate aminotransferase (AST), creatinine (Crea), urea, total cholesterol (TC), low-density lipoprotein cholesterol (LDL-C), high-density lipoprotein cholesterol (HDL-C), and triglycerides (TG) were determined using the corresponding assay kits on a BS-420 automatic biochemical analyzer (Mindray, Shenzhen, China). At the same time, kidney, liver, and pancreas tissues in each group of mice were collected and fixed in 4% paraformaldehyde for H&E staining. Immunohistochemistry analyses for insulin in pancreas sections were performed with an Expose mouse-specific AP detection IHC kit (dilution ratio = 1:1000, Abcam, Cambridge, UK).

Statistical Analysis. All data are presented as the means ± SEM. In the in vitro GLP-1R activation experiment, data were analyzed using a sigmoid function (Hill model) to calculate the EC_{50} values of each sample (n = 3). The trapezoidal rule was used to determine the AUC values of the glucose profiles. Differences among groups were analyzed using one-way or two-way analysis of variance (ANOVA), followed by Dunnett's post hoc multiple comparison test. Differences with P values <0.05 were considered statistically significant. Statistical analysis and plotting were performed with GraphPad Prism 6.0 (GraphPad Software Inc., San Diego, CA, USA).

■ ASSOCIATED CONTENT

Supporting Information

The Supporting Information is available free of charge at https://pubs.acs.org/doi/10.1021/acs.jmedchem.1c00032.

Analytical data and characterizations of native Ex4, Ex4-LPETGGS (peptide 1), FITC-labeled Ex4-LPETGGS (peptide 2), and conjugate 6−11; standard curve of the cAMP concentration using competitive cAMP ELISA, peptide 2 and conjugate 9−11 generated by fluorescence reading, and DNP moiety concentration as a function of optical density; ELISA results of the binding activity between Ex4−DNP conjugates and anti-DNP antibodies; quantitative analysis of immunostaining for insulin; flow cytometry evaluation of the HEK293-GLP1-R-AcGFP cell construction; procedure and protocol for the expression and purification of SrtA in *Escherichia coli* BL21 (DE3); preparation of DNP-carrier protein conjugates; ELISA protocol for DNP-antibody titer determination; ELISA protocol for determination of the binding activity between Ex4−DNP conjugates and anti-DNP antibodies or preimmunized mouse serum; and HEK293-GLP1-R-AcGFP construction (PDF)

■ AUTHOR INFORMATION

Corresponding Authors

Lei Nie − *Hisun Biopharmaceutical Co., Limited, 311404 Hangzhou, Zhejiang, China*; Email: lei_nie@126.com

Zhimeng Wu − *Key Laboratory of Carbohydrate Chemistry & Biotechnology, Ministry of Education, School of Biotechnology, Jiangnan University, 214122 Wuxi, China*; orcid.org/0000-0001-7583-7268; Phone: 86-51085197582; Email: zwu@jiangnan.edu.cn; Fax: 86-51085197582

Authors

Shijie Dai − *Key Laboratory of Carbohydrate Chemistry & Biotechnology, Ministry of Education, School of Biotechnology, Jiangnan University, 214122 Wuxi, China*

Haofei Hong − *Key Laboratory of Carbohydrate Chemistry & Biotechnology, Ministry of Education, School of Biotechnology, Jiangnan University, 214122 Wuxi, China*

Kun Zhou − *Key Laboratory of Carbohydrate Chemistry & Biotechnology, Ministry of Education, School of Biotechnology, Jiangnan University, 214122 Wuxi, China*

Kai Zhao − *Key Laboratory of Carbohydrate Chemistry & Biotechnology, Ministry of Education, School of Biotechnology, Jiangnan University, 214122 Wuxi, China*

Yuntian Xie − *Key Laboratory of Carbohydrate Chemistry & Biotechnology, Ministry of Education, School of Biotechnology, Jiangnan University, 214122 Wuxi, China*

Chen Li − *Key Laboratory of Carbohydrate Chemistry & Biotechnology, Ministry of Education, School of Biotechnology, Jiangnan University, 214122 Wuxi, China*

Jie Shi − *Key Laboratory of Carbohydrate Chemistry & Biotechnology, Ministry of Education, School of Biotechnology, Jiangnan University, 214122 Wuxi, China*

Zhifang Zhou − *Key Laboratory of Carbohydrate Chemistry & Biotechnology, Ministry of Education, School of Biotechnology, Jiangnan University, 214122 Wuxi, China*

Complete contact information is available at: https://pubs.acs.org/10.1021/acs.jmedchem.1c00032

Notes

The authors declare no competing financial interest.

■ ACKNOWLEDGMENTS

This work was supported by the National Natural Science Foundation of China (nos. 21907038 and 32000904), Natural Science Foundation of Jiangsu Province (no. BK20200601), China Postdoctoral Science Foundation (no. BX20200153),

and Jiangsu Key Research and Development Plan (BE2019632). This work was partly supported by the Health and Family Planning Commission of Wuxi, China (no. Z202005), the Basic Research Program of Jiangnan University (no. JUSRP12016), the 111 Project (no. 111-2-06), the Open Foundation of Key Laboratory of Carbohydrate Chemistry & Biotechnology Ministry of Education (no. 202006), and the National First-class Discipline Program of Food Science and Technology (JUFSTR20180101).

■ ABBREVIATIONS

T2DM, type 2 diabetes mellitus; GLP-1, glucagon-like peptide 1; AUC, area under the curve; FcRn, neonatal Fc-receptor; nADAs, neutralizing antidrug antibodies; SML, sortase A-mediated ligation; PEG, polyethylene glycol; SAR, structure−activity relationship; SPPS, solid-phase peptide synthesis; cAMP, cyclic adenosine monophosphate; HEK293, human embryonic kidney 293; Ahx, aminocaproic acid; PK, pharmacokinetic; ELISA, enzyme-linked immunosorbent assay; H&E, hematoxylin-eosin; FDA, Food and Drug Administration; ALT, alanine aminotransferase; AST, aspartate aminotransferase; $T_{1/2}$, half-life; TC, total cholesterol; TG, serum triglycerides; LDL-C, low-density lipoprotein cholesterol; HDL-C, high-density lipoprotein cholesterol; HbA1c, hemoglobin A1c; FBG, fasting blood glucose

■ REFERENCES

(1) American Diabetes Association. 2. Classification and Diagnosis of Diabetes: Standards of Medical Care in Diabetes-2020. *Diabetes Care* **2020**, *43*, S14−S31.
(2) Magliano, D. J.; Islam, R. M.; Barr, E. L. M.; Gregg, E. W.; Pavkov, M. E.; Harding, J. L.; Tabesh, M.; Koye, D. N.; Shaw, J. E. Trends in incidence of total or type 2 diabetes: systematic review. *BMJ* **2019**, *366*, l5003.
(3) Suzuki, R.; Brown, G. A.; Christopher, J. A.; Scully, C. C. G.; Congreve, M. Recent Developments in Therapeutic Peptides for the Glucagon-like Peptide 1 and 2 Receptors. *J. Med. Chem.* **2020**, *63*, 905−927.
(4) Koliaki, C.; Doupis, J. Incretin-based therapy: a powerful and promising weapon in the treatment of type 2 diabetes mellitus. *Diabetes Ther.* **2011**, *2*, 101−121.
(5) Drucker, D. J. Mechanisms of Action and Therapeutic Application of Glucagon-like Peptide-1. *Cell Metab.* **2018**, *27*, 740−756.
(6) Meier, J. J. GLP-1 receptor agonists for individualized treatment of type 2 diabetes mellitus. *Nat. Rev. Endocrinol.* **2012**, *8*, 728−742.
(7) Christensen, M.; Miossec, P.; Larsen, B.; Werner, U.; Knop, F. The design and discovery of lixisenatide for the treatment of type 2 diabetes mellitus. *Expert Opin. Drug Discovery* **2014**, *9*, 1223.
(8) Sai, W.; Tian, H.; Yang, K.; Tang, D.; Bao, J.; Ge, Y.; Song, X.; Zhang, Y.; Luo, C.; Gao, X.; Yao, W. Systematic Design of Trypsin Cleavage Site Mutated Exendin4-Cysteine 1, an Orally Bioavailable Glucagon-Like Peptide-1 Receptor Agonist. *Int. J. Mol. Sci.* **2017**, *18*, 578.
(9) Han, J.; Huang, Y.; Chen, X.; Zhou, F.; Fei, Y.; Fu, J. Rational design of dimeric lipidated Xenopus glucagon-like peptide 1 analogues as long-acting antihyperglycaemic agents. *Eur. J. Med. Chem.* **2018**, *157*, 177−187.
(10) Lau, J.; Bloch, P.; Schäffer, L.; Pettersson, I.; Spetzler, J.; Kofoed, J.; Madsen, K.; Knudsen, L. B.; McGuire, J.; Steensgaard, D. B.; Strauss, H. M.; Gram, D. X.; Knudsen, S. M.; Nielsen, F. S.; Thygesen, P.; Reedtz-Runge, S.; Kruse, T. Discovery of the Once-Weekly Glucagon-Like Peptide-1 (GLP-1) Analogue Semaglutide. *J. Med. Chem.* **2015**, *58*, 7370−7380.
(11) Han, J.; Sun, L.; Chu, Y.; Li, Z.; Huang, D.; Zhu, X.; Qian, H.; Huang, W. Design, synthesis, and biological activity of novel dicoumarol glucagon-like peptide 1 conjugates. *J. Med. Chem.* **2013**, *56*, 9955−9968.
(12) Qi, Y.; Simakova, A.; Ganson, N. J.; Li, X.; Luginbuhl, K. M.; Ozer, I.; Liu, W.; Hershfield, M. S.; Matyjaszewski, K.; Chilkoti, A. A brush-polymer conjugate of exendin-4 reduces blood glucose for up to five days and eliminates poly(ethylene glycol) antigenicity. *Nat. Biomed. Eng.* **2017**, *1*, 0002.
(13) Kong, J.-H.; Oh, E. J.; Chae, S. Y.; Lee, K. C.; Hahn, S. K. Long acting hyaluronate−exendin 4 conjugate for the treatment of type 2 diabetes. *Biomaterials* **2010**, *31*, 4121−4128.
(14) Dai, S.; Liu, S.; Li, C.; Zhou, Z.; Wu, Z. Site-selective modification of exendin 4 with variable molecular weight dextrans by oxime-ligation chemistry for improving type 2 diabetic treatment. *Carbohydr. Polym.* **2020**, *249*, 116864−116872.
(15) Ning, L.; He, B.; Zhou, P.; Derda, R.; Huang, J. Molecular Design of Peptide-Fc Fusion Drugs. *Curr. Drug Metab.* **2019**, *20*, 203−208.
(16) Roopenian, D. C.; Akilesh, S. FcRn: the neonatal Fc receptor comes of age. *Nat. Rev. Immunol.* **2007**, *7*, 715−725.
(17) Heath, C.; Pettit, D. "Fc Fusion Proteins". *Challenges in Protein Product Development*; Springer, 2018; pp 545−558.
(18) Schmidt, S. *Fusion Protein Technologies for Biopharmaceuticals. Applications and Challenges*; Wiley, 2013.
(19) Imai, K.; Takaoka, A. Comparing antibody and small-molecule therapies for cancer. *Nat. Rev. Cancer* **2006**, *6*, 714−727.
(20) Levin, D.; Golding, B.; Strome, S. E.; Sauna, Z. E. Fc fusion as a platform technology: potential for modulating immunogenicity. *Trends Biotechnol.* **2015**, *33*, 27−34.
(21) Liu, L. Pharmacokinetics of monoclonal antibodies and Fc-fusion proteins. *Protein Cell* **2018**, *9*, 15−32.
(22) Umpierrez, G.; Tofé Povedano, S.; Pérez Manghi, F.; Shurzinske, L.; Pechtner, V. Efficacy and Safety of Dulaglutide Monotherapy Versus Metformin in Type 2 Diabetes in a Randomized Controlled Trial (AWARD-3). *Diabetes Care* **2014**, *37*, 2168−2176.
(23) Perdomo, M. F.; Levi, M.; Sällberg, M.; Vahlne, A. Neutralization of HIV-1 by redirection of natural antibodies. *Proc. Natl. Acad. Sci. U.S.A.* **2008**, *105*, 12515−12520.
(24) Sheridan, R. T. C.; Hudon, J.; Hank, J. A.; Sondel, P. M.; Kiessling, L. L. Rhamnose glycoconjugates for the recruitment of endogenous anti-carbohydrate antibodies to tumor cells. *Chembiochem* **2014**, *15*, 1393−1398.
(25) Rullo, A. F.; Fitzgerald, K. J.; Muthusamy, V.; Liu, M.; Yuan, C.; Huang, M.; Kim, M.; Cho, A. E.; Spiegel, D. A. Re-engineering the Immune Response to Metastatic Cancer: Antibody-Recruiting Small Molecules Targeting the Urokinase Receptor. *Angew. Chem., Int. Ed.* **2016**, *55*, 3642−3646.
(26) McEnaney, P. J.; Parker, C. G.; Zhang, A. X.; Spiegel, D. A. Antibody-recruiting molecules: an emerging paradigm for engaging immune function in treating human disease. *ACS Chem. Biol.* **2012**, *7*, 1139−1151.
(27) Feigman, M. J. S.; Pires, M. M. Synthetic Immunobiotics: A Future Success Story in Small Molecule-Based Immunotherapy? *ACS Infect. Dis.* **2018**, *4*, 664−672.
(28) Uvyn, A.; De Geest, B. G. Multivalent Antibody-Recruiting Macromolecules: Linking Increased Binding Affinity with Enhanced Innate Immune Killing. *Chembiochem* **2020**, *21*, 3036−3043.
(29) Hong, H.; Zhou, Z.; Zhou, K.; Liu, S.; Guo, Z.; Wu, Z. Site-specific C-terminal dinitrophenylation to reconstitute the antibody Fc functions for nanobodies. *Chem. Sci.* **2019**, *10*, 9331−9338.
(30) Li, S.; Yu, B.; Wang, J.; Zheng, Y.; Zhang, H.; Walker, M. J.; Yuan, Z.; Zhu, H.; Zhang, J.; Wang, P. G.; Wang, B. Biomarker-Based Metabolic Labeling for Redirected and Enhanced Immune Response. *ACS Chem. Biol.* **2018**, *13*, 1686−1694.
(31) Nagano, M.; Carrillo, N.; Otsubo, N.; Hakamata, W.; Ban, H.; Fuller, R. P.; Bashiruddin, N. K.; Barbas, C. F., 3rd In vivo programming of endogenous antibodies via oral administration of adaptor ligands. *Bioorg. Med. Chem.* **2017**, *25*, 5952−5961.
(32) Yu, B.; Hwang, D.; Jeon, H.; Kim, H.; Lee, Y.; Keum, H.; Kim, J.; Lee, D. Y.; Kim, Y.; Chung, J.; Jon, S. A Hybrid Platform Based on

https://doi.org/10.1021/acs.jmedchem.1c00032
J. Med. Chem. 2021, 64, 4947−4959

a Bispecific Peptide-Antibody Complex for Targeted Cancer Therapy. *Angew. Chem., Int. Ed.* **2019**, *58*, 2005−2010.
(33) Schmidt, D. H.; Kaufman, B. M.; Butler, V. P. Persistence of hapten antibody complexes in the circulation of immunized animals after a single intravenous injection of hapten. *J. Exp. Med.* **1974**, *139*, 278−294.
(34) Ortega, E.; Kostovetzky, M.; Larralde, C. Natural DNP-binding immunoglobulins and antibody multispecificity. *Mol. Immunol.* **1984**, *21*, 883−888.
(35) Farah, F. S. Natural antibodies specific to the 2, 4 dinitrophenyl group. *Immunology* **1973**, *25*, 217−226.
(36) Wu, Z.; Guo, Z. Sortase-Mediated Transpeptidation for Site-Specific Modification of Peptides, Glycopeptides, and Proteins. *J. Carbohydr. Chem.* **2012**, *31*, 48−66.
(37) Tsukiji, S.; Nagamune, T. Sortase-mediated ligation: a gift from Gram-positive bacteria to protein engineering. *Chembiochem* **2009**, *10*, 787−798.
(38) Göke, R.; Fehmann, H. C.; Linn, T.; Schmidt, H.; Krause, M.; Eng, J.; Göke, B. Exendin-4 is a high potency agonist and truncated exendin-(9-39)-amide an antagonist at the glucagon-like peptide 1-(7-36)-amide receptor of insulin-secreting beta-cells. *J. Biol. Chem.* **1993**, *268*, 19650−19655.
(39) Heath, C.; Pettit, D. *"Fc Fusion Proteins"*; Springer, 2018; pp 545−558.
(40) Sathish, J. G.; Sethu, S.; Bielsky, M.-C.; de Haan, L.; French, N. S.; Govindappa, K.; Green, J.; Griffiths, C. E. M.; Holgate, S.; Jones, D.; Kimber, I.; Moggs, J.; Naisbitt, D. J.; Pirmohamed, M.; Reichmann, G.; Sims, J.; Subramanyam, M.; Todd, M. D.; Van Der Laan, J. W.; Weaver, R. J.; Park, B. K. Challenges and approaches for the development of safer immunomodulatory biologics. *Nat. Rev. Drug Discovery* **2013**, *12*, 306−324.
(41) Chen, X.; Zaro, J. L.; Shen, W.-C. Pharmacokinetics of recombinant bifunctional fusion proteins. *Expert Opin. Drug Metab. Toxicol.* **2012**, *8*, 581−595.
(42) Yap, M. K. K.; Misuan, N. Exendin-4 from Heloderma suspectum venom: From discovery to its latest application as type II diabetes combatant. *Basic Clin. Pharmacol. Toxicol.* **2019**, *124*, 513−527.
(43) Furman, B. L. The development of Byetta (exenatide) from the venom of the Gila monster as an anti-diabetic agent. *Toxicon* **2012**, *59*, 464−471.
(44) Muttenthaler, M.; King, G. F.; Adams, D. J.; Alewood, P. F. Trends in peptide drug discovery. *Nat. Rev. Drug Discovery* **2021**, *20*, 309−325.
(45) Palasek, S. A.; Cox, Z. J.; Collins, J. M. Limiting racemization and aspartimide formation in microwave-enhanced Fmoc solid phase peptide synthesis. *J. Pept. Sci.* **2007**, *13*, 143−148.
(46) Cheng, X.; Zhu, T.; Hong, H.; Zhou, Z.; Wu, Z. Sortase A-mediated on-resin peptide cleavage and in situ ligation: an efficient one-pot strategy for the synthesis of functional peptides and proteins. *Org. Chem. Front.* **2017**, *4*, 2058−2062.
(47) Luginbuhl, K. M.; Schaal, J. L.; Umstead, B.; Mastria, E. M.; Li, X.; Banskota, S.; Arnold, S.; Feinglos, M.; D'Alessio, D.; Chilkoti, A. One-week glucose control via zero-order release kinetics from an injectable depot of glucagon-like peptide-1 fused to a thermosensitive biopolymer. *Nat. Biomed. Eng.* **2017**, *1*, 0078.
(48) Zhou, Z.; Mandal, S. S.; Liao, G.; Guo, J.; Guo, Z. Synthesis and Evaluation of GM2-Monophosphoryl Lipid A Conjugate as a Fully Synthetic Self-Adjuvant Cancer Vaccine. *Sci. Rep.* **2017**, *7*, 11403.
(49) Zhong, X.; Chen, Z.; Chen, Q.; Zhao, W.; Chen, Z. Novel Site-Specific Fatty Chain-Modified GLP-1 Receptor Agonist with Potent Antidiabetic Effects. *Molecules* **2019**, *24*, 779.

https://doi.org/10.1021/acs.jmedchem.1c00032
J. Med. Chem. 2021, 64, 4947−4959